Chalcogenide Letters Vol. 22, No. 11, November 2025, p. 987 - 995

CdS nanoparticles-Loaded 1D attapulgite Composites for Boosting Photocatalytic Activity

Xiaowang Lu[1,*], Cheng Luo[1], Xinyu Zhu[1], Ziwen Gu[1], Chen Da[1], Junyan Zhou[1] and Junchao Qian[2]

[1]School of Materials Engineering, Yancheng Institute of Technology, Yancheng, 224051, China
[2]School of Material Science and Engineering, Suzhou University of Science and Technology, Suzhou 215009, China
*Corresponding author: Xiaowang Lu. Email: luxiaowang@ycit.edu.cn

Received: 24 July 2025; Accepted: 26 November 2025

ABSTRACT: Attapulgite clay-supported CdS composites were synthesized via hydrothermal approach and applied to remove Rhodamine B (RhB). The structural, morphological, and physicochemical properties of the materials were systematically characterized by XRD, TEM, XPS, BET and UV-Vis DRS. The combination of CdS and attapulgite could enhance active site availability and surface area, thereby boosting photocatalytic activity.The optimized CdS/attapulgite composite demonstrated remarkable photocatalytic efficiency under visible-light illumination. In addition, a potential photocatalytic degradation mechanism by the composites was proposed.

KEYWORDS: CdS; Attapulgite; Photocatalyst; Photocatalytic degradation

1 Introduction

As the industrial economy has developed, the textile printing and dyeing industry has also experienced rapid growth. However, the production process of this industry discharges a large amount of dye waste water, causing severe pollution to the environment. This makes the purification of dye-contaminated water extremely important. Multiple approaches have been established for the treatment of dye-laden effluents, such as activated carbon adsorption, semiconductor photocatalytic technology, ultrafiltration, reverse osmosis, biodegradation, etc. [1–5]. Among various approaches, semiconductor photocatalysis demonstrates distinctive merits for organic dye decomposition owing to its facile synthesis, economic viability and eco-friendly characteristics.

Therefore, it is imperative to develop photocatalysts with exceptional photocatalytic efficiency. Owing to their unique optoelectronic and catalytic properties coupled with relatively stable chemical characteristics. metal chalcogenide semiconductors have been extensively investigated. CdS is a prototypical visible-light-responsive photocatalyst that has attracted significant attention due to its optimal band structure and stable phase composition. However, pristine CdS exhibits limited photocatalytic efficiency owing to its constrained active surface area, tendency for particle agglomeration, and electron-hole pairs generated by photoexcitation quickly recombine, which severely restricts its practical applications [6,7].

Attapulgite (ATP) is a naturally occurring hydrated silicate mineral characterized by its distinctive layer-chain structure and nanofibrous morphology [8]. This mineral is cost-effective, chemically stable, and exhibits exceptional adsorption capacity owing to its well-developed internal channel system [9,10]. Furthermore, attapulgite possesses an extensive specific surface area combined with numerous active sites, making it an ideal supporting matrix for loading various metal chalcogenides to construct functional composite materials.

In this study, CdS nanoparticles were employed to decorate one-dimensional attapulgite for the fabrication of CdS/ATP nanocomposites. And then photocatalytic activities of the prepared materials were assessed by decomposing organic dyes under visible-light illumination. Finally, the underlying mechanism for organic dye photodegradation was thoroughly elucidated.

https://doi.org/10.15251/CL.2025.2211.987

2 Experimental

2.1 Synthesis of the Composite

0.2 g attapulgite powder was homogeneously distributed throughout 60 mL deionized water by agitation, and the mixture was ultrasonically treated for half an hour. Then, A stoichiometric amount of cadmium acetate and sodium sulfide was introduced into the suspension under continuous stirring for 2 h. After transferring the mixture into a 100 mL PTFE-lined hydrothermal reactor, it was heated to and maintained at 180°C for 12 h, followed by filtration, washing, and drying to obtain the CdS/ATP composite material by changing the amounts of the $Cd(CH_3COO)_2$ and Na_2S, the weight percentages of CdS loaded on attapulgite were set at 10%, 20%, 30%, 40%, and 50%.

2.2 Characterization

A DX-2700 XRD analyzer was used for structural characterization. Morphological analysis was conducted via transmission electron microscopy (TEM, JEM-2100). Surface composition was determined by XPS (ESCALAB 250). Optical properties were evaluated through UV-Vis DRS measurements (UV-2450) and BET surface area was measured by an Autosorb-1 analyzer.

2.3 Photocatalytic Activity

In a typical procedure, the photocatalyst (100 mg) was uniformly mixed into a 100 mL aqueous solution of RhB (10 mg/L) light-protected Shaking for 0.5 h for adsorption. Subsequently, the suspension was carefully moved to a temperature-regulated chamber and exposed to a 300 W xenon lamp with visible light-transmitting optical filter. At 20-min intervals, a 5 mL suspension sample was collected. Then the sample was centrifuged at 6000 rpm to to separate solid particulates. The supernatant was analyzed using a UV-Vis spectrometer, measuring the concentration of RhB at its maximum absorption wavelength (554 nm). The degradation efficiency was calculated by the equation:

$$D\% = [(C_0 - C_t)/C_0] \times 100\% \quad (1)$$

with C_0 and C_t corresponding to the starting and time-dependent concentrations, respectively.

3 Results and Discussion

3.1 XRD Analysis

Structural evolution from individual components (ATP and CdS) to composite materials with designed CdS loading levels was systematically analyzed by XRD, as demonstrated in Fig. 1. The characteristic peaks near 8.5°, 19.8°, 28.1° and 35.0° can be identified (110), (400), (040), (440) lattice planes of attapulgite (PDF#29-0855). In the case of bare CdS, the main diffraction peaks at 24.7°, 26.5°,43.7° and 51.9°are indexed as the (100), (002), (110), (112) lattice planes of hexagonal CdS (PDF# 06-0314), respectively. The successful deposition of CdS nanoparticles on ATP is confirmed by the preservation of characteristic diffraction peaks from both hexagonal CdS and attapulgite in the composite materials. While the concentration of CdS increases, the characteristic diffraction peak intensity of attapulgite at 8.5° gradually decreases and which of CdS gradually increases. The results demonstrate the successful preparation of CdS/ATP composite.

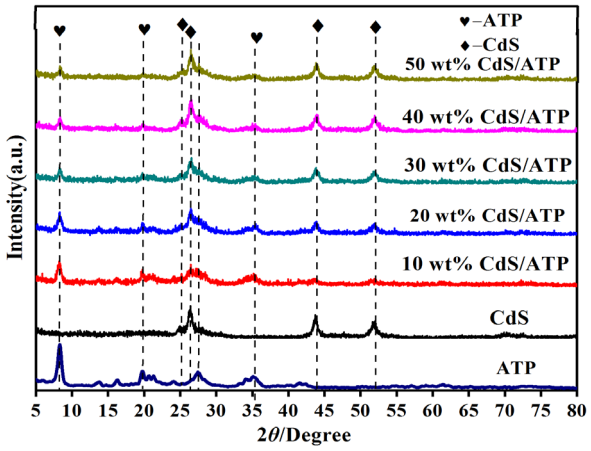

Figure 1: XRD patterns of ATP, CdS, and CdS/ATP composites.

3.2 TEM Analysis

The TEM image of 40wt% CdS/ATP composite is shown in Fig. 2a. The ATP exhibits a fibrous morphology with diameters ranging from 20 to 60 nm. The ATP fibers maintain their structural integrity after CdS nanoparticle deposition, with the nanoparticles being uniformly dispersed on their surfaces The EDS spectrum (Fig. 2b) confirmed that 40wt% CdS/ATP composite contains Si, Mg, Al, Cd and S. These results demonstrate that CdS nanoparticles are successfully immobilized on the attapulgite substrate, forming a composite material.

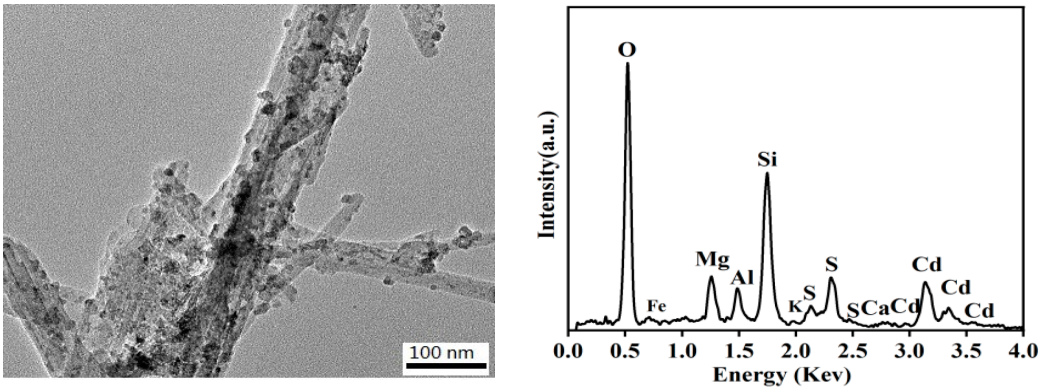

(a) **(b)**

Figure 2: (**a**) TEM image of 40wt% CdS/ATP composite and (**b**) EDS spectrum.

3.3 XPS Analysis

The XPS analysis was conducted to thoroughly investigate the 40wt% CdS/ATP composite, aiming to obtain more precise understanding of the elemental valence states. As shown in Fig. 3a, two characteristic peaks can be observed at the position of 404.9 eV (Cd $3d_{5/2}$) and 411.8 eV (Cd $3d_{3/2}$), which verifies the Cd^{2+} state in CdS. Similarly, the S 2p spectrum (Fig. 3b) reveals the doublet located at 162.2 eV and 163.0 eV, corresponding to S $2p_{3/2}$ and S $2p_{1/2}$ respectively, which clearly indicates the presence of S^{2-} anions in CdS [11,12]. Additionally, the Si 2p spectrum (Fig. 3c) displays a binding energy of 102.2 eV, consistent with the Si-O framework of attapulgite [13]. These results collectively demonstrate the successful formation of CdS/ATP composites.

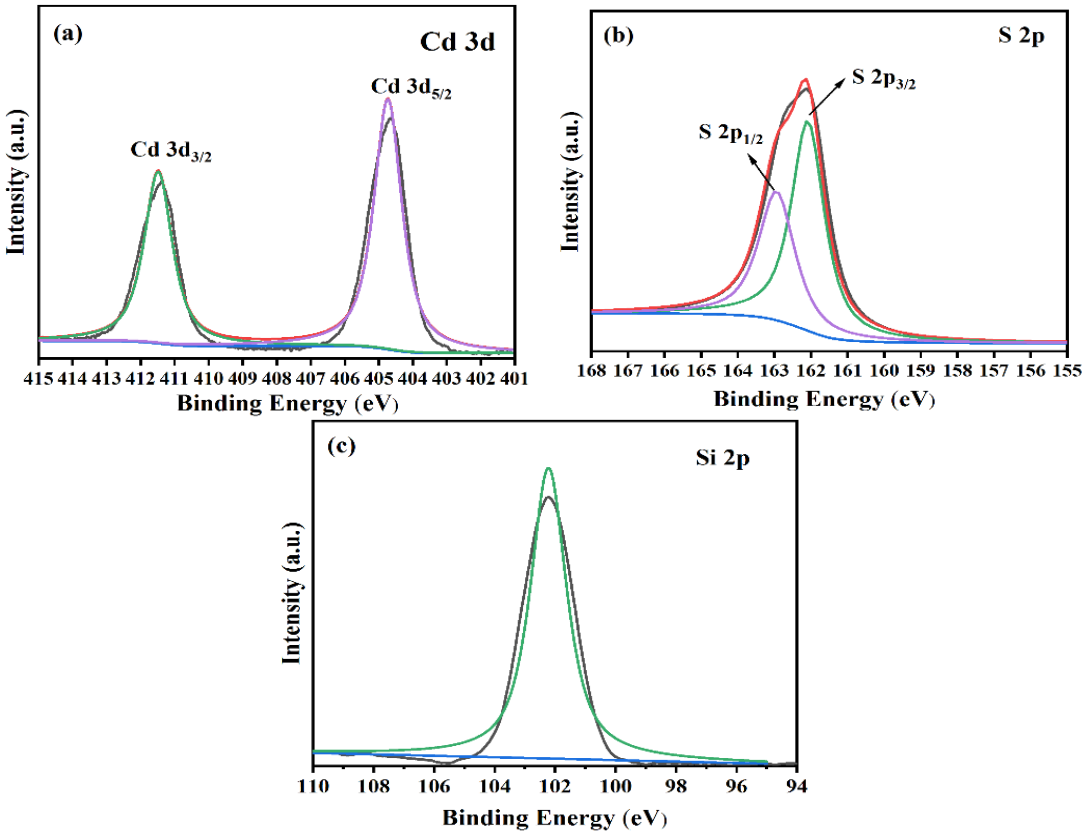

Figure 3: XPS spectra of 40 wt% CdS/ATP composite (**a**) Cd 3d, (**b**) S 2p, and (**c**) Si 2p.

3.4 BET Analysis

BET analysis serves as one of the essential methods for characterizing photocatalytic activity. As shown in Fig. 4, pure ATP and 40wt% CdS/ATP exhibit type IV isothermal adsorption-desorption curves, indicating their mesoporous adsorption characteristics [14,15]. According to Table 1, after loading CdS onto the ATP surface, both the surface area and hole capacity increased significantly. These facilitates the adsorption of RhB molecules and enhances light-harvesting capability, thereby improving photocatalytic efficiency.

Table 1: BET data for ATP and 40 wt% CdS/ATP.

Material	Surface Area/(m^2/g)	Hole Capacity/(m^3/g)
ATP	120.5	0.37
40wt% CdS/ATP	182..6	0.52

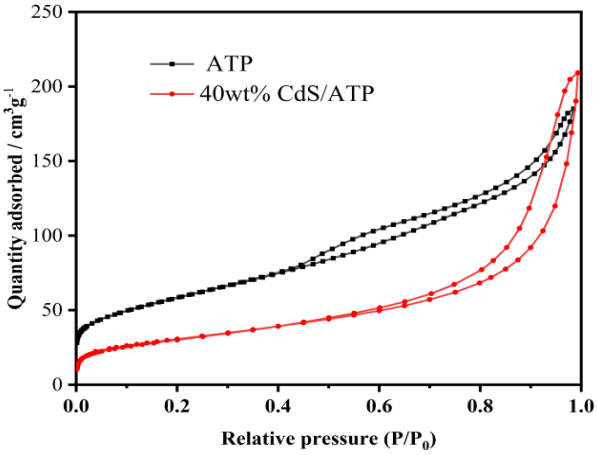

Figure 4: N_2 adsorption-desorption isotherm of ATP and 40wt% CdS/ATP composite.

3.5 DRS Analysis

Fig. 5a confirms that the absorption spectra of CdS and CdS/ATP composites are predominantly located within the visible light range, while demonstrating gradually strengthened light absorption and a slight red shift of the light absorption edge with increasing CdS loading. The optical bandgaps (E_g) of the CdS/ATP composites were determined using the Tauc plot method [16,17]. Bandgap analysis via Tauc plots presented in Fig. 5b, calculated from the spectral data in Fig. 5a. The extrapolated linear regions yield E_g values ranging from 2.25 eV to 2.35 eV for the CdS/ATP composites, confirming their visible-light absorption capability.

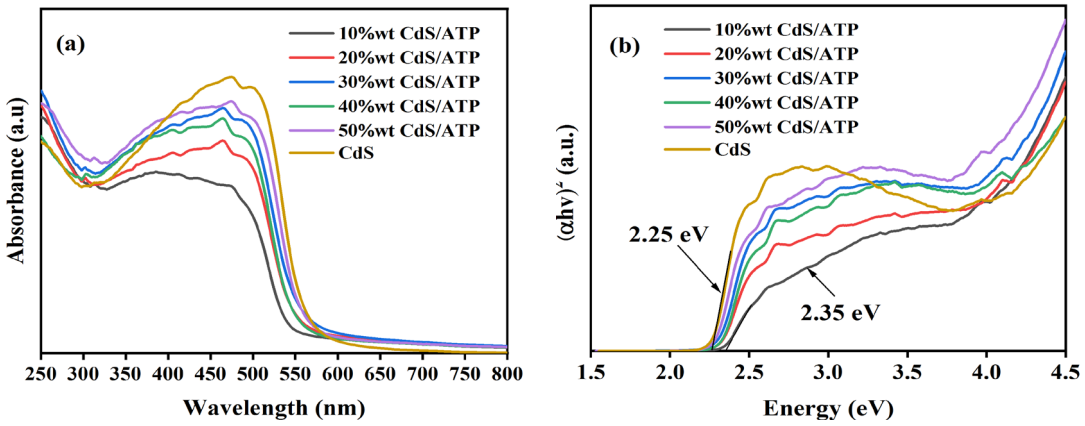

Figure 5: (**a**) UV-Vis DRS of CdS/ATP composites; (**b**) the corresponding band gap widths.

3.6 Photocatalytic Activity

RhB solution was selected as the target pollutant to evaluate the photocatalytic performance of CdS and CdS/ATP composites (Fig. 6a). In the dark period, all the samples show some degradation of RhB (about 10%), which is mainly due to the minor amount adsorption of attapulgite. Owing to synergistic effects, the CdS/ATP composite demonstrates significantly enhanced photocatalytic activity toward RhB degradation relative to its individual components (pure attapulgite and pure CdS). Notably, 40wt% CdS/ATP composite achieves the best RhB removal efficiency, with a degradation rate of 92% in 2 h under visible light irradiation. At its core, this phenomenon results from that the combination of CdS and attapulgite can richer active sites accompanied by enlarged specific surface, which is beneficial for improving photocatalytic performance [18]. The RhB degradation kinetics followed first-order kinetics

[19,20], with the corresponding kinetic curves presented in Fig. 6b. The 40wt% CdS/ATP composite achieves an RhB degradation rate constant (k) of 0.018 min^{-1}, representing 2.6-fold and 18-fold enhancements over pure CdS and pure attapulgite, respectively. Time-resolved Ultraviolet-visible spectroscopy (Fig. 6c) served to monitor the attenuation of RhB's characteristic absorption peak during photocatalytic degradation by the 40 wt% CdS/ATP composite. The marked reduction in the maximum absorbance of RhB is ascribed to deethylation processes, demonstrating that the photodegradation of RhB involves both deethylation and breakdown of the chromophoric structure [21,22]. The photocatalytic stability has been thoroughly examined through multiple degradation cycles. Fig. 6d illustrates the results of five cycles of RhB degradation using 40wt% CdS/ATP composite. The outcomes demonstrated that the 40wt% CdS/ATP photocatalyst is effectively recycled for 5 runs without a significant drop in photodegradation, indicating the good stability.

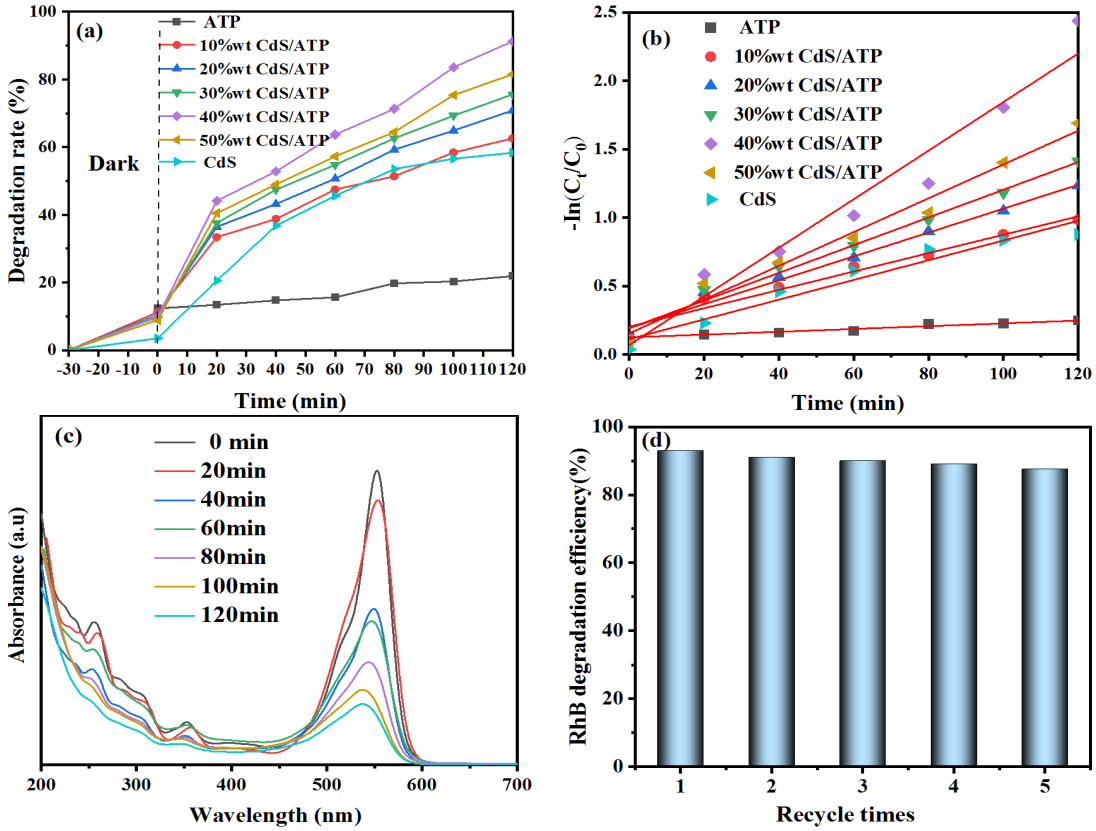

Figure 6: (**a**) RhB degradation curves, (**b**) and corresponding kinetic curves of samples for RhB, (**c**) RhB temporal UV–vis absorption spectrum, (**d**) Reusability of 40wt% CdS/ATP composite for degradation of RhB.

3.7 Photocatalytic Mechanism

The primary reactive species involved in conventional photocatalytic dye degradation include h^+, •OH, and $•O_2^-$. In the 40wt% CdS/ATP photocatalytic system for RhB degradation, the corresponding scavengers triethanolamine (TEOA), tert-butyl alcohol (TBA) and benzoquinone (BQ) were sequentially added to quench these reactive species [23,24]. Fig. 7 shows the scavenger effects in photocatalysis. The $•O_2^-$ serves as the predominant active species, while holes (h^+) play a secondary role and hydroxyl radicals (•OH) show negligible involvement in RhB photodegradation. As a result, CdS can be activated when the composite is irradiated under visible light, and the charge carriers (electrons and holes) are produced. Electrons migrating through conduction band have the capability to efficiently combine with molecular oxygen in the system, leading to the formation of superoxide radicals ($•O_2^-$), which is a strong oxidizing agent species that degrades RhB molecules. Furthermore, the active holes on the valence band can direct-

ly oxidize organic pollutants. Meanwhile, attapulgite can quickly aggregate dye molecules around photocatalysts and increase a large number of active sites, serving as an efficient co-catalyst, improve photocatalytic activity. Eventually, the organic pollutant RhB is oxidized to small molecules including CO_2 and H_2O for degradation.

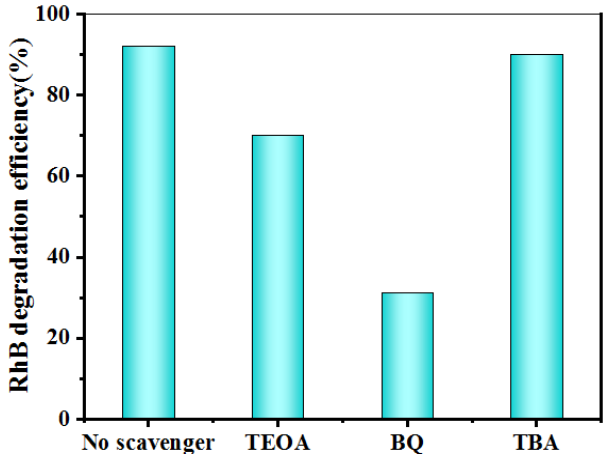

Figure 7: Scavenger experiment of 40wt% CdS/ATP composite for RhB degradation.

4 Conclusions

The CdS/ATP composites are successfully prepared by hydrothermal method. Attapulgite as a carrier can provide more active sites and increase specific surface area for photocatalytic degradation. Notably, with 40wt% CdS nanoparticles deposition, the CdS/ATP composite displays superior photocatalytic capability, and the degradation rate of RhB reaches 92% within the visible spectrum. Additionally, the cyclic experiments of CdS/ATP compositehave confirmed that the 40 wt% composite has practical recyclability and photostability. The $\bullet O_2^-$ serves as the predominant active species, while holes (h^+) play a secondary role and hydroxyl radicals (•OH) show negligible involvement in RhB photodegradation. Therefore, the synergistic effect of CdS and attapulgite can effectively enhance photocatalytic activity.

Acknowledgement: Not applicable.

Funding Statement: This research was funded by School-level Research Projects of Yancheng Institute of Technology, grant number:xjr2019026. The APC was funded also by School-level Research Projects of Yancheng Institute of Technology.

Author Contributions: Study conception and design: Lu Xiaowang, Qian Junchao; data collection: Luo Cheng and Zhu Xinyu; analysis and interpretation of results: Gu Ziwen, Da Chen, Zhou Junyan; draft manuscript preparation: Lu Xiaowang, Luo Cheng, Zhu Xinyu.

Availability of Data and Materials: Data available on request from the authors.

Ethics Approval: Not applicable.

Conflicts of Interest: The authors declare no conflicts of interest to report regarding the present study

References

1. Han N, Xu QX, Beyene G, Zhang QF. Enhanced photocatalytic activity over g-C3N4/(BiO)2(OH) Cl2− Z-scheme heterojunction. Appl Surf Sci. 2020;521:146464. https://doi.org/10.1016/j.apsusc.2020.146464
2. Liu TT, Zhou YL, Zheng WX, Chang CG, Dong JM, Wen J, et al. FeS/MgO-biochar composites for boosting the adsorption-photocatalytic degradation of RhB. Mater Sci Semicond Process. 2024;174:108178. https://doi.org/10.1016/j.mssp.2024.108178

3. Kang YH, Kwon J, Kim JB, Hong SK. Fate of low molecular weight organic matters in reverse osmosis and vacuum ultraviolet process for high-quality ultrapure water production in the semiconductor industry. J Cleaner Prod. 2023;423:138714. https://doi.org/10.1016/j.jclepro.2023.138714
4. Hu RX, Liu Y, Zhu GJ, Chen C, Hantoko D, Yan M. COD removal of wastewater from hydrothermal carbonization of food waste: Using coagulation combined activated carbon adsorption. J Water Process Eng. 2022;45:102462. https://doi.org/10.1016/j.jwpe.2021.102462
5. Zumstein M, Battagliarin G, Kuenke A, Sander M. Environmental Biodegradation of Water-Soluble Polymers: Key Considerations and Ways Forward. Acc Chem Res. 2022;55:2163. https://doi.org/10.1021/acs.accounts.2c00232
6. Ren YJ, Li YF, Pan GX, Wang N, Xing Y, Zhang ZY. Recent progress in CdS-based S-scheme photocatalysts. J Mater Sci Technol. 171,162 (2024); https://doi.org/10.1016/j.jmst.2023.06.052
7. Tu BY, Hao JR, Wang FH, Li YF, Li JN, Qiu JL. Element doping adjusted the built-in electric field at the TiO2/CdS interface to enhance the photocatalytic reduction activity of Cr(VI). Chem Eng J. 2023;456:141103. https://doi.org/10.1016/j.cej.2022.141103
8. Zhang TT, Wang W, Zhao YL, Bai HY, Wen T, Kang SC, et al. Removal of heavy metals and dyes by clay-based adsorbents: From natural clays to 1D and 2D nano-composites. Chem Eng J. 2021;420:127574. https://doi.org/10.1016/j.cej.2020.127574
9. Li XZ, Zhu W, Lu XW, Zuo SX, Yao C, Ni CY. Integrated nanostructures of CeO2/attapulgite/g-C3N4 as efficient catalyst for photocatalytic desulfurization: Mechanism, kinetics and influencing factors. Chem Eng J. 2017;326:87. https://doi.org/10.1016/j.cej.2017.05.131
10. Wei XF, Li W, Fan XQ, Zhu MH. MoS2-functionalized attapulgite hybrid toward high-performance thickener of lubricating grease. Tribol Int. 2023;179:108135. https://doi.org/10.1016/j.triboint.2022.108135
11. Wang ZD, Chen YF, Zhang LY, Cheng B, Yu JG, Fan JJ. Step-scheme CdS/TiO_2 nanocomposite hollow microsphere with enhanced photocatalytic CO2 reduction activity. J Mater Sci Technol. 2020;56:143. https://doi.org/10.1016/j.jmst.2020.02.062
12. Li CQ, Du X, Jiang S, Liu Y, Niu ZL, Liu ZY, et al. Constructing Direct Z-Scheme Heterostructure by Enwrapping $ZnIn_2S_4$ on CdS Hollow Cube for Efficient Photocatalytic H_2 Generation. Adv Sci. 2022;9:2201773. https://doi.org/10.1002/advs.202201773
13. Qi YZ, Zhao SK, Jiang XY, Kang ZK, Gao SL, Liu WG, et al. Visible-Light-Driven BiOBr-TiO_2-Attapulgite Photocatalyst with Excellent Photocatalytic Activity for Multiple Xanthates. Catalysts. 2023;13:1504. https://doi.org/10.3390/catal13121504
14. Zhang ZF, Gui WJ, Wei J, Cui YJ, Li P, Jia ZL, et al. Functionalized Attapulgite for the Adsorption of Methylene Blue: Synthesis, Characterization, and Adsorption Mechanism. ACS Omega. 2021;6:19586. https://doi.org/10.1021/acsomega.1c02111
15. Yang HM, ADT, Ouyang J, Li M, Mann S. From Natural Attapulgite to Mesoporous Materials: Methodology, Characterization and Structural Evolution. J Phys Chem B 2010;114:2390. https://doi.org/10.1021/jp911516b
16. Lu XW, Li XZ, Chen F, Chen ZG, C Qian J, Zhang QF. Biotemplating synthesis of N-doped two-dimensional CeO_2–TiO_2 nanosheets with enhanced visible light photocatalytic desulfurization performance. J Alloys Compd. 2020;815:152326. https://doi.org/10.1016/j.jallcom.2019.152326
17. Mou RM, Liu Z, Zhang DL, Yang AL. Enhanced visible light induced photocatalytic degradation of oxytetracycline hydrochloride by n-ZnO/p-NiO composite. Chem Phys Lett. 2023;829:140741. https://doi.org/10.1016/j.cplett.2023.140741
18. Zhang GX, Li SL, Li YF, Dong XB. 2D/1D ZnIn2S4/attapulgite hybrid materials for enhanced photocatalytic performance under visible light. Appl Clay Sci. 2023;246:107162. https://doi.org/10.1016/j.clay.2023.107162
19. Hu L, Wang ZW, Shi YZ, Liu C, Hou YD, Bi JH, et al. Coordination activation enhanced photocatalytic performance for levofloxacin degradation over defect-rich WO_3 nanosheets. J Environ Chem Eng. 2022;10:108738. https://doi.org/10.1016/j.jece.2022.108738
20. Li YJ, Sun SG, Ma MY, Ouyang YZ, Yan WB. Kinetic study and model of the photocatalytic degradation of rhodamine B (RhB) by a TiO_2-coated activated carbon catalyst: Effects of initial RhB content, light intensity and TiO2 content in the catalyst. Chem Eng J. 2008;142:147. https://doi.org/10.1016/j.cej.2008.01.009
21. Madima N, Kefeni KK, Mishra SB, Mishra AK, Kuvarega AT. Fabrication of magnetic recoverable Fe3O4/TiO2 heterostructure for photocatalytic degradation of rhodamine B dye. Inorg Chem Commun. 2022;145:109966. https://doi.org/10.1016/j.inoche.2022.109966
22. Bikerchalen S, Akhsassi B, Bakiz B, Villain S, Taoufyq A, Guinneton F, et al. Photocatalytic degradation of Rhodamine B dye over oxygen-rich bismuth oxychloride Bi24O31Cl10 photocatalyst under UV and Visible light irradiation: Pathways and mechanism. J Phys Chem Solids. 2025;196:112342. https://doi.org/10.1016/j.jpcs.2024.112342

23. Wang H, Qiu XQ, Liu WF, Yang DJ. Facile preparation of well-combined lignin-based carbon/ZnO hybrid composite with excellent photocatalytic activity. Appl Surf Sci. 2017;426:206. https://doi.org/10.1016/j.apsusc.2017.07.112
24. Wu SH, Yu X, Zhang JL, Zhang YM, Zhu Y, Zhu MH. Construction of BiOCl/CuBi2O4 S-scheme heterojunction with oxygen vacancy for enhanced photocatalytic diclofenac degradation and nitric oxide removal. Chem Eng J. 2021;411:128555. https://doi.org/10.1016/j.cej.2021.128555